

**Electronic Supporting Information**

**Sustainable porous carbons from tannic acid based KOH activated as high-performance CO<sub>2</sub> capture sorbents**

*Yujia Zhang<sup>a</sup>, Fengwu Tian<sup>a</sup>, Xiaosha Guo<sup>a</sup>, Miaomiao Bai<sup>a</sup>, Tian Tang<sup>a</sup>, Xixi Di<sup>a</sup>, Wei Wang<sup>a</sup>, Zhifeng Liu<sup>a,b</sup>, Xianzhao Shao<sup>a,\*</sup>*

*<sup>a</sup>Shaanxi Key Laboratory of Catalysis, School of Chemistry and Environment Science, Shaanxi University of Technology, Hanzhong 723001, China;*

*<sup>b</sup>State Key Laboratory of Qinba Bio-Resource and Ecological Environment, Shaanxi University of Technology, Hanzhong 723001, Shaanxi, China*

\* Corresponding authors. E-mail addresses: xianzhaoshao@snut.edu.cn (X. Shao)

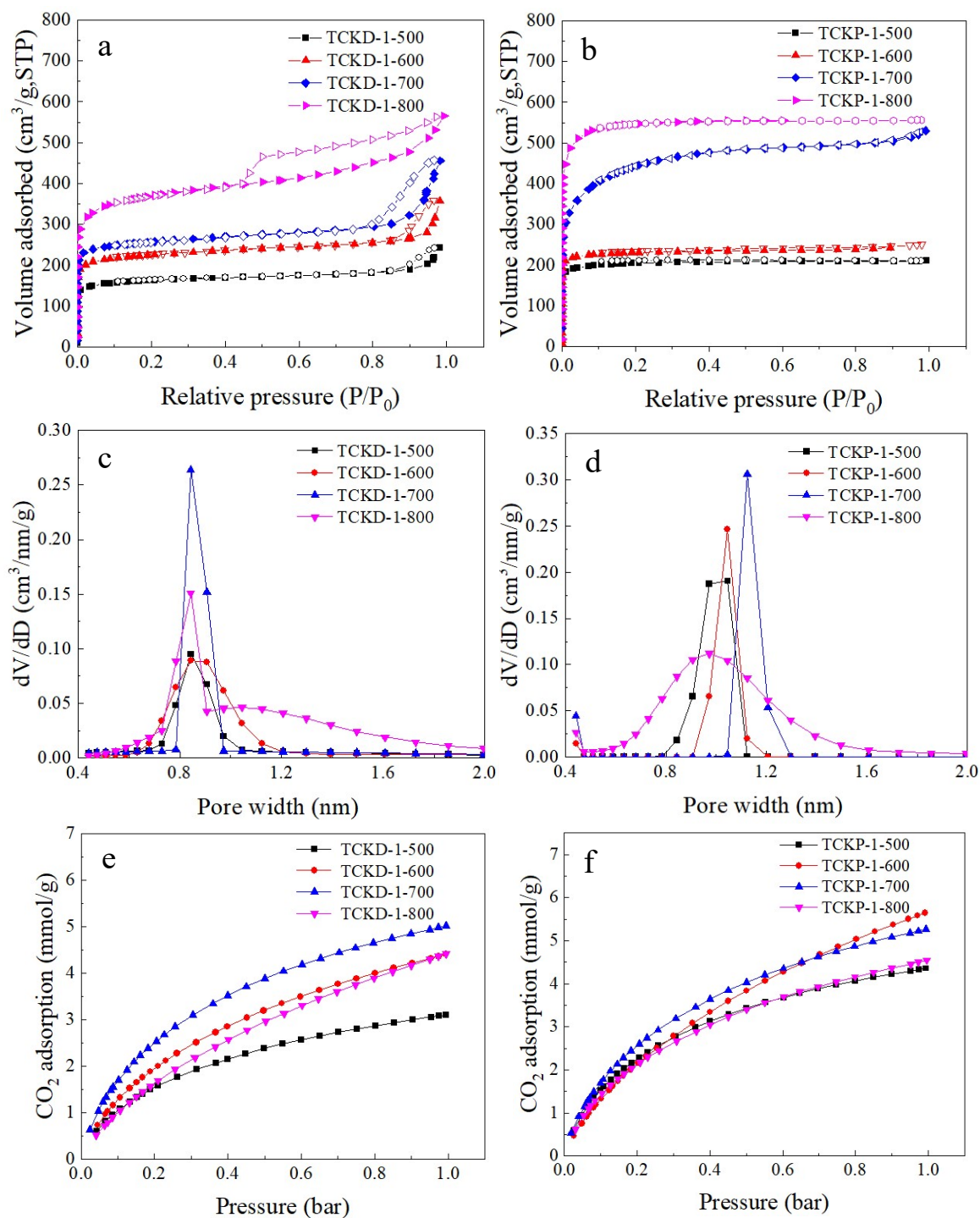


**Figure S1.** (a-b) Comparison of TCKs-1-Y obtained at different activation temperature by gas adsorption/desorption analysis. (a-b) N<sub>2</sub> sorption isotherms at -196 °C, (c-d) pore size distribution (PSD), PSD was calculated by NLDFT with the slit pore geometry assumption. (e-f) CO<sub>2</sub> adsorption isotherms at 0 °C

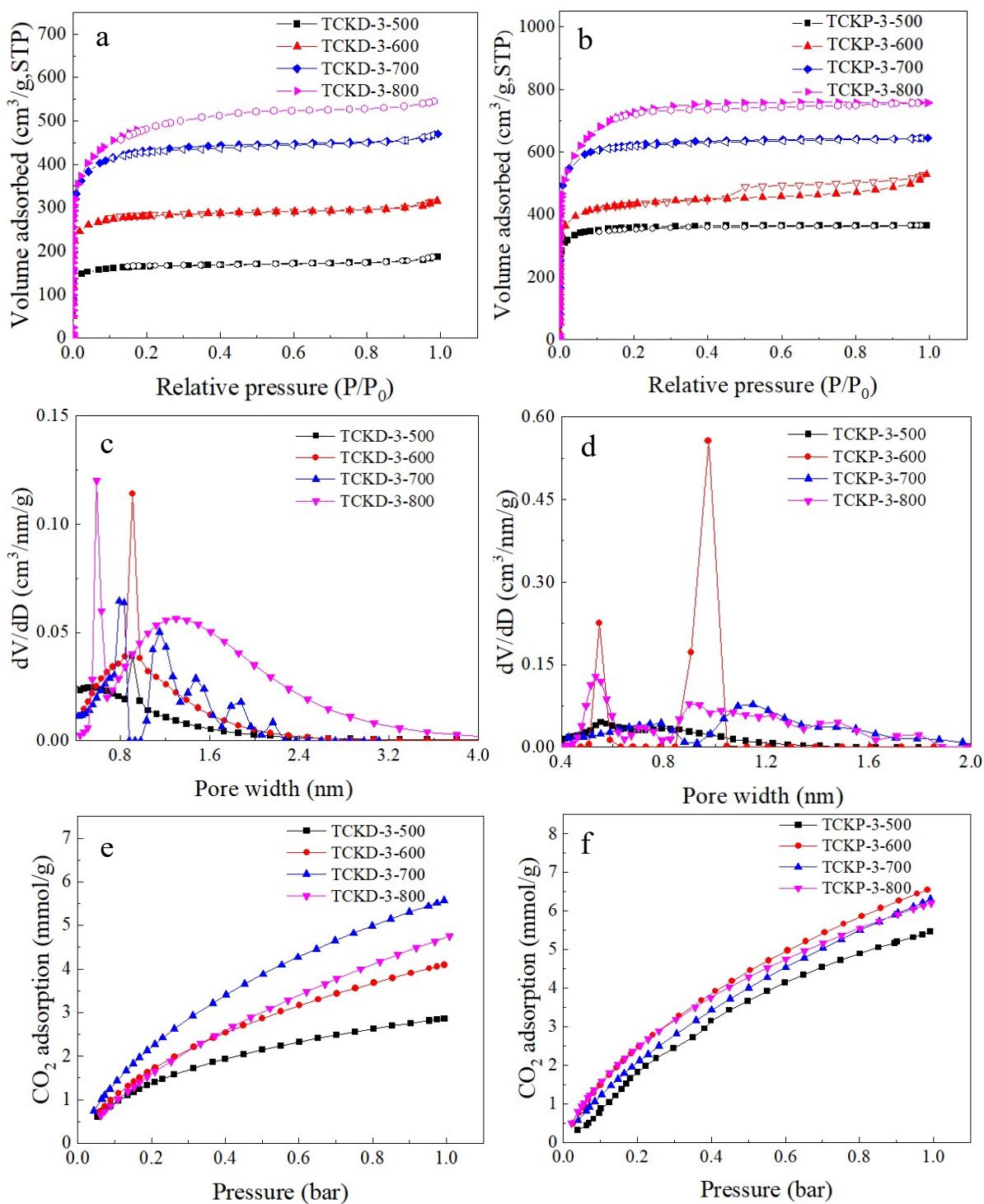


**Figure S2.** (a-b) Comparison of TCKs-3-Y obtained at different activation temperature by gas adsorption/desorption analysis. (a-b) N<sub>2</sub> sorption isotherms at -196 °C, (c-d) pore size distribution (PSD), PSD was calculated by NLDFT with the slit pore geometry assumption. (e-f) CO<sub>2</sub> adsorption isotherms at 0 °C

## S1. Supplementary experimental section

### *The application of Ideal adsorbed solution theory (IAST) for calculating adsorption selectivity of CO<sub>2</sub>/N<sub>2</sub>*

The adsorption selectivity is a significant parameter to evaluate the adsorption separation efficiency in the industrial processes. The adsorption selectivity of TCKs for CO<sub>2</sub>/N<sub>2</sub> binary mixture is defined as Eq. (S1).

$$S = \frac{x_1}{x_2} \times \frac{y_2}{y_1} \quad (\text{Eq.S1})$$

Where  $x_i$  and  $y_i$  represent the mole fraction of component  $i$  ( $i=1$  or  $2$ ) in the adsorbed and bulk phases, respectively. In this work, component 1 represents CO<sub>2</sub>, while component 2 represents N<sub>2</sub>. Ideal adsorbed solution theory (IAST) is widely applied to predict the adsorption selectivities of binary gas mixtures from pure component isotherms, which is based on the principle that the adsorbate-adsorbent and adsorbate-adsorbate interactions are sufficiently ideal. In addition, an appropriate model used to fit pure-component isotherm is important to compute the integration required by IAST. Although there are no constraints on the choice of IAST models, the data should be fit precisely over the full range of pressure.

In this work, the experimentally measured loadings for CO<sub>2</sub> were measured as a function of the absolute pressure at two different temperatures 273 and 298 K. The CO<sub>2</sub> isotherm for were fitted with the Single-site Langmuir-Freundlich model.

$$q = q_{sat} \frac{bp^v}{1+bp^v} \quad (\text{Eq.S2})$$

Where  $q$  is the adsorbed amount in equilibrium with the concentration of adsorbate in the gas phase (mmol/g),  $p$  is the equilibrium pressure of the bulk gas with the adsorbed phase (kPa);  $q_{sat}$  is the saturation capacities of CO<sub>2</sub> or N<sub>2</sub> (mmol/g);  $b$  is the affinity coefficients of CO<sub>2</sub> or N<sub>2</sub> (1/kPa), respectively; and  $v$  is equal to  $1/n_1$ ,  $t$  is equal to  $1/n_2$ , where  $n_1$  and  $n_2$  are the corresponding deviations from an ideal homogeneous surface. The Single-site Langmuir-Freundlich model was combined with the Ideal adsorbed solution theory (IAST) to predict the adsorption isotherms of the mixture and calculate the selectivity of the adsorbate.

**Table S1.** Single-site Langmuir-Freundlich parameters for adsorption of CO<sub>2</sub> in different TCKP-2-600 and TCKD-2-700.

Sample	$q_{sat}$ mmol/g	$b_0$ Pa <sup>-<math>\nu</math></sup>	$\nu$ dimensionless
TCKP-2-600	6.37828	1.26621	1.00928
TCKD-2-700	6.84578	0.91067	1.19419

**Table S2.** Single-site Langmuir-Freundlich parameters for adsorption of N<sub>2</sub> in different TCKP-2-600 and TCKD-2-700.

Sample	$q_{sat}$ mmol/g	$b_0$ Pa <sup>-<math>\nu</math></sup>	$\nu$ dimensionless
TCKP-2-600	3.91529	0.12787	0.96746
TCKD-2-700	4.23783	0.06446	1.00227

**Table S3.** CO<sub>2</sub> adsorption performance of TCKP-2-600 and other adsorbents.

Biomass	Sample	Preparation method	CO <sub>2</sub> uptake (mmol/g at 1 bar)		S <sub>BET</sub> (m <sup>2</sup> /g)	V <sub>mic</sub> (cm <sup>3</sup> /g)	CO <sub>2</sub> /N <sub>2</sub> Selectivity	Serial number	References
			0 °C	25 °C					
Olive stones	OS	single-step activation	4.8	3.0	1113	0.37	18	S1	[1]
Almond shells	AS	single-step activation	3.7	2.7	822	0.33	20	S2	[1]
Pomegranate peels	PP	single-step activation	6.03	4.11	585	0.20	15.1	S3	[2]
Carrot peels	CP	single-step activation	5.64	4.18	1379	0.51	8.1	S4	[2]
Fern leaves	FL	single-step activation	4.52	4.12	1593	0.54	5.6	S5	[2]
Rice Husk	-	single-step activation	-	3.10	1492	0.34	7.6	S6	[3]
Coffee grounds	CG800-1	single-step activation	7.18	4.54	1692	0.68	17	S7	[4]
Amazonian nutshells	BNS	single-step activation	5.14	3.67	1532	0.44	46.9	S8	[5]
Arundo donax	KLB2	single-step activation	6.3	3.6	1122	0.50	-	S9	[6]
Coconut Shell	C-600-3	carbonization and KOH activation	6.04	4.23	1172	0.43	22	S10	[7]
Microcrystalline cellulose	ACel-ac	carbonization and KOH activation	5.8	3.7	753	0.27	-	S11	[8]
Chestnut shell	WS-600-0.6	carbonization and KOH activation	5.23	3.61	1255	0.48	16	S12	[9]
Vine shoots	BC-CO <sub>2</sub> -0.1-800	carbonization and CO <sub>2</sub> activation	3.45	1.10	374	0.112	55.2	S13	[10]
Vine shoots	AC-KOH-W-2-600	carbonization and KOH activation	6.04	1.21	1305	0.451	44.2	S14	[10]
Vine shoots	AC-KOH-D-5-700	carbonization and KOH activation	6.08	1.98	1439	0.493	58.8	S15	[10]
Wheat	MCC-K3	carbonization and KOH activation	5.7	3.48	1438	0.581	16	S16	[11]
Lotus seed	LSB3-800	carbonization and KOH activation	6.8	3.1	2230	0.67	-	S17	[12]
Peanut shell	PC680	carbonization and KOH activation	7.25	4.41	1713	0.73	7.9	S18	[13]
Fungi	PC-2	carbonization and KOH activation	5.5	3.4	1742	-	18.5	S19	[14]
Sawdust	AS-2-600	carbonization and KOH activation	6.1	4.8	1260	0.55	5.4	S20	[15]
Coffee grounds	NCLK3	carbonization and KOH activation	4.7	3.0	840	0.36	13	S21	[16]
Africa palm Shells	C600K3	carbonization and KOH activation	6.3	4.4	1250	0.55	-	S22	[17]
Polyurethane foam	PUF-400-KOH-1-700	N-doped activated	6.67	4.33	1516	0.57	12	S23	[18]
Fir bark	ACBK3	N-doped activated	7.0	5.2	1377	0.51	32.3	S24	[19]
Rice husk	CAC-5	N-doped activated	5.83	3.68	1495	0.447	15.3	S25	[20]
Phenolic resin	RUK-600-3	N-doped activated	7.13	4.61	1404	0.53	12	S26	[21]
Arundo donax	NDAB3-500	N-doped activated	3.6	2.1	1863	0.32	-	S27	[22]
Alligator Weed	NAB800-2	N-doped activated	6.4	5.4	3031	0.58	-	S28	[23]
Lotus stalk	LSC-500-1	N-doped activated	5.62	3.88	1113	0.41	22	S29	[24]
Tannic acid	TCKP-2-600	carbonization and KOH activation	7.03	4.29	1845	0.74	20.3		<b>This work</b>

## References

- [1]. A.S. González, M.G. Plaza, F. Rubiera, C. Pevida, Sustainable biomass-based carbon adsorbents for post-combustion CO<sub>2</sub> capture, *Chem. Eng. J.* 230 (2013) 456-465.
- [2]. J. Serafin, U. Narkiewicz, A.W. Morawski, R.J. Wróbel, B. Michalkiewicz, Highly microporous activated carbons from biomass for CO<sub>2</sub> capture and effective micropores at different conditions, *J. CO<sub>2</sub> Util.* 18 (2017) 73-79.
- [3]. M. Li, R. Xiao, Preparation of a dual Pore Structure Activated Carbon from Rice Husk Char as an Adsorbent for CO<sub>2</sub> Capture, *React. Fuel-Process. Technol.* 186 (2019) 35-39.
- [4]. M.J. Kim, S.W. Choi, H. Kim, S. Mun, K.B. Lee, Simple synthesis of spent coffee ground-based microporous carbons using K<sub>2</sub>CO<sub>3</sub> as an activation agent and their application to CO<sub>2</sub> capture, *Chem. Eng. J.* 397 (2020) 1385-8947.
- [5]. J. Serafin, M. Ouzzine, O.F. C. Junior, J. Sreńscek-Nazzal, Preparation of low-cost activated carbons from amazonian nutshells for CO<sub>2</sub> storage, *Biomass Bioenerg* 144 (2021) 0961-9534.
- [6]. G. Singh, I.Y. Kim, K.S. Lakhi, P. Srivastava, R. Naidu, A. Vinu, Single step synthesis of activated bio-carbons with a high surface area and their excellent CO<sub>2</sub> adsorption capacity, *Carbon* 116 (2017) 448-455.
- [7]. J. Yang, L. Yue, X. Hu, O.L. Wang, Y. Zhao, Y. Lin, Y. Sun, H. DaCosta, L.P. Guo, Efficient CO<sub>2</sub> Capture by Porous Carbons Derived from Coconut Shell, *Energy Fuels* 31 (2017) 4287-4293.
- [8]. R.S. Dassanayake, C. Gunathilake, T. Jackson, Preparation and adsorption properties of aerocellulose-derived activated carbon monoliths. *Cellulose* 23 (2016) 1363-1374.
- [9]. C. Quan, R. Su, N.B. Gao, Preparation of activated biomass carbon from pine sawdust for supercapacitor and CO<sub>2</sub> capture, *Int J Energy Res.*3 (2020) 1-17.
- [10]. J.J. Manyà, B. González, M. Azuara, G. Arner, Ultra-microporous adsorbents prepared

- from vine shoots-derived biochar with high CO<sub>2</sub> uptake and CO<sub>2</sub>/N<sub>2</sub> selectivity, *Chem. Eng. J.* 345 (2018) 631-639.
- [11]. S.M. Hong, E. Jang, A. Dysart, CO<sub>2</sub> Capture in the Sustainable Wheat-Derived Activated Microporous Carbon Compartments, *Sci Rep* 6 (2016) 34590.
- [12]. G. Singh, K.S. Lakhi, K. Ramadass, C.I. Sathish, A. Vinu, High-Performance Biomass-Derived Activated Porous Biocarbons for Combined Pre- and Post-Combustion CO<sub>2</sub> Capture, *ACS Sustainable Chem. Eng.* 7 (2019) 7412-7420.
- [13]. D. Li, Y. Tian, L. Li, Production of highly microporous carbons with large CO<sub>2</sub> uptakes at atmospheric pressure by KOH activation of peanut shell char, *J Porous Mater* 22 (2015) 1581-1588.
- [14]. J.C. Wang, A. Heerwig, Ma.R. Lohe, M. Oschatz, L. Borchardt, S. Kaskel, Fungi-based porous carbons for CO<sub>2</sub> adsorption and separation, *J. Mater. Chem.* 22 (2012) 13911-13913.
- [15]. M. Sevilla, A.B. Fuertes, Sustainable porous carbons with a superior performance for CO<sub>2</sub> capture, *Energy Environ. Sci.* 4 (2011) 1765-1771.
- [16]. M.G. Plaza, A.S. González, C. Pevida, J.J. Pis, F. Rubiera, Valorisation of spent coffee grounds as CO<sub>2</sub> adsorbents for postcombustion capture applications, *At. Energ.* 99 (2012) 272-279.
- [17]. A. S. Ello, L.K. Souza, A. Trokourey, M. Jaroniec, Development of microporous carbons for CO<sub>2</sub> capture by KOH activation of African palm shells, *J. CO<sub>2</sub> Util.* 2013 (2) 35-38.
- [18]. C. Ge, J. Song, Z.F. Qin, J.G. Wang, W.B. Fan, Polyurethane Foam-Based Ultramicroporous Carbons for CO<sub>2</sub> Capture, *ACS Appl. Mater. Interfaces* 8 (2016) 18849-18859.



- [19]. L. Luo, T. Chen, Z. Li, Z. Zhang, W. Zhao, M. Fan, Heteroatom self-doped activated biocarbons from fir bark and their excellent performance for carbon dioxide adsorption, *J. CO<sub>2</sub> Util.* 25 (2018) 89-98.
- [20]. S. He, G.Y. Chen, H. Xiao, G.B. Shi, C.C. Ruan, Y.S. Ma, H.M. Dai, B.H. Yuan, X.F. Chen, X.B. Yang, Facile preparation of N-doped activated carbon produced from rice husk for CO<sub>2</sub> capture, *J. Colloid Interface Sci.* 582 (2021) 90-101.
- [21]. L.M. Yue, L.L. Rao, L.L. Wang, Y. Sun, Z.Z. Wu, H. DaCosta, X. Hu, Enhanced CO<sub>2</sub> Adsorption on Nitrogen-Doped Porous Carbons Derived from Commercial Phenolic Resin, *Energy Fuels* 32 (2) (2018) 2081-2088.
- [22]. G. Singh, I.Y. Kim, K.S. Lakhi, S. Joseph, P. Srivastava, R. Naidu, A. Vinu, Heteroatom functionalized activated porous biocarbons and their excellent performance for CO<sub>2</sub> capture at high pressure, *J. Mater. Chem. A.* 5 (2017) 21196-21204.
- [23]. G. Singh, R. Bahadur, J.M. Lee, I.Y. Kim, A.M. Ruban, J.M. Davidraj, D. Semit, A. Karakoti, H.A. Muhtaseb, A. Vinu, Nanoporous activated biocarbons with high surface areas from alligator weed and their excellent performance for CO<sub>2</sub> capture at both low and high pressures, *Chem. Eng. J.* 406 (2021) 1385-8947.
- [24]. L.L. Rao, L. Yue, L.L. Wang, Z.Z. Wu, C.D. Ma, L.Y. An, X. Hu, Low-Temperature and Single-Step Synthesis of N-Doped Porous Carbons with a High CO<sub>2</sub> Adsorption Performance by Sodium Amide Activation, *Energy Fuels* 32 (10) (2018) 10830-10837.